IMPELMENTATION AND DIFFERENCES BETWEEN BLOOD RHEOLOGICAL MODELS IN SIMULATING THE FLOW IN AN ABDOMINAL AORTIC ANEURYSM

P. Neofytou[*], S. Tsangaris[†] and M. Kyriakidis[**]

[*,†]School of Mechanical Engineering, Fluids Section, National Technical University of Athens, 15780 Zografou, Athens, Greece

[**]Medical School, Department of Cardiology, University of Athens, Laikon Hospital, 11527 Goudi, Athens, Greece.

[†]email: sgt@fluid.mech.ntua.gr

A numerical study of the flow-induced effects by different blood constitutive equations is carried out utilising a three-dimensional model of an abdominal aortic aneurysm. Three non-Newtonian models are employed, namely the Casson, Power-Law and Quemada models, which have been introduced in the past for modelling the rheological behaviour of blood. The three-dimensional flow field and in particular the pressure difference as well as both low and high values of the wall shear stress in the vicinity of the aneurysm are investigated and a comparison is made between the effects of each rheological model on the aforementioned parameters. Results show marked differences between simulating blood as Newtonian and as non-Newtonian fluid and furthermore that the Power-Law exhibits the highest sensitivity to any parametric change followed gradually by the Casson and Quemada models.

1 INTRODUCTION

The development of an Abdominal Aortic Aneurysm (AAA) is a very serious condition induced by localized bulging of the vessel the normal diameter of which is around 2cm. Continuous dilation of the wall may lead to AAAs with diameter of up to 5cm the most severe outcome of which is rupture of the AAA. The latter occurs when the stress within the aneurysm wall exceeds the tensile strength of the wall thus posing an extremely high risk of fatality. Furthermore the presence of the AAA itself may lead to flow disturbances such as vortex formation, which is reported as a contributing factor to atherogenesis and thrombogenesis [1]. The role of hemodynamics in the growth and potential rupture of aneurysms and the induced flow disturbances that may lead to other anomalies in the arterial network have been under investigation for many years.

Studies of AAAs in particular have been performed by Yu *et al.* [2] who investigated the steady and pulsatile flow characteristics in axisymmetric AAA models using a commercial Computational Fluid Dynamics (CFD) package. A later study by Yu [3] was solely focused on the experimental investigation of the steady and pulsatile flow in a AAA model using Particle Image Velocimetry. The study covered different model geometries as well as different Reynolds and Womersley numbers. Egelhoff *et al.* [4] investigated both experimentally and numerically the flow in AAA models during resting and exercise conditions and showed that no vortex formation takes place in small AAAs whereas vortex formation and transition to turbulence takes place in moderate size AAAs under exercise conditions. Transition to turbulence was also addressed in a similar experimental study by Salsac *et al.* [5] who also investigated the magnitude of wall shear stress during progressive enlargement of AAAs. Numerical flow predictions in AAAs were also performed by Viswanathan *et al*. [6] who used a more sophisticated AAA model covering different geometrical parameters and confirmed that mechanical forces on the arterial wall caused by the blood flow may play an important role in both development and growth of aneurysms.

The aim of the present study is to investigate the effects of modelling the blood as non-Newtonian fluid for 3D flows in an aneurysm as done in the past for 2D flows in stenosis models [7] employing three well documented blood rheological models namely the Casson Power-Law and Quemada [9] models. The investigation is carried out by numerically modelling the flow in a 3D axisymmetric model of an AAA at different Reynolds numbers and degrees of AAA dilation.

2 MODEL

2.1 Governing equations

The flow is considered laminar and incompressible and therefore the Navier-Stokes equations for three-dimensional incompressible flow are used in their integral form in order to accommodate the subsequent finite-volume discretisation. Following the analysis in [7] the shear-stress tensor in the diffusion terms is expressed in the case of non-Newtonian fluids as

$$\bar{\tau} = \mu(|\bar{\gamma}|)\bar{\gamma} \qquad (1)$$

where $\bar{\dot{\gamma}}$ is the shear-rate tensor and μ is the viscosity expressed as a function of the second invariant of $\bar{\dot{\gamma}}$. The dimensionless expression of this equation yields the characteristic flow parameters for every model:

(*i*) Casson model: The Reynolds and Bingham numbers

$$\mathrm{Re}_{\mathrm{CA}} = \frac{\rho U_\infty D}{\mu_\infty}, \quad \mathrm{Bi} = \frac{\tau_y D}{\mu_\infty U_\infty} \tag{2}$$

are the characteristic parameters for a Casson-model flow.

(*ii*) Power-Law model: The Reynolds number defined as

$$\mathrm{Re}_{\mathrm{PL}} = \frac{\rho D^n}{k U_\infty^{n-2}} \tag{3}$$

is characteristic parameter for a Power-Law-model flow.

(*iii*) Quemada model: The dimensionless parameters

$$\mathrm{Re}_{\mathrm{QU}} = \frac{\rho U_\infty D}{\mu_F}, \quad \gamma_c^* = \frac{\gamma_c}{U_\infty / D} \tag{4}$$

are the characteristic parameters for a Quemada-model flow.

2.2 Geometry

The geometry consists of a tube of diameter D and can be divided in three segments namely the inlet segment with length 4D, the aneurysm segment with length b=4D and the outlet segment with length 18D. The radius R_0 of the inlet and outlet segments is undeformed and equal to D/2, whereas the radius of the segment is given by

$$R = R_0 + \left(a - R_c + \sqrt{R_c^2 - \left[b/2 - x \right]^2} \right), \; 0 \le x \le b \tag{5}$$

where $R_c = \dfrac{a^2 + (b/2)^2}{2a}$ and a is the maximum width of the dilated segment. . For the current study, three different values of a were used namely 0.25, 0.4 and 0.55, the shape of which is shown in Figure 1.

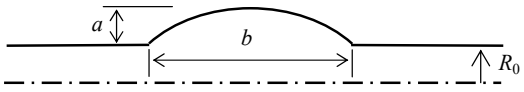

Fig. 1. Geometrical model of the vessel with the aneurysm.

2.3 Conditions and parameters

Apart from the different values of a, the effects of the blood rheological models under consideration are studied for different Reynolds numbers. These are Re=300, 900 and 1500. Due the fact that the Navier-Stokes equations are incorporated into the numerical scheme in their dimensionless form, the characteristic parameters in equations (2), (3) and (4) are to be calculated accordingly. For the Casson model and according to Charm *et al.* [11] for blood, τ_y=10.82mPa, μ_∞=3.1·10^{-3}Pa·s and ρ=1056kg/m^3. In addition, D=2cm was considerd in compliance with blood flow in AAAs [4]. Therefore, from $\mathrm{Re}_{\mathrm{CA}}$ having the same definition as Re for Newtonian flows, the calculation of U_∞ from each of the aforementioned values of Re is possible and thus Bi can be calculated. For the Power-Law model the parameters in (3) according to Walburn and Schneck [8] are in the case of blood k=14.67·10^{-3}Pa·s^n and n=0.7755. Therefore according to calculation of U_∞, for each value of Re the corresponding value of $\mathrm{Re}_{\mathrm{PL}}$ can be calculated. The parameters of Quemada model for blood [9] are γ_c=1.88s^{-1}, k_∞=2.07 and k_o=4.33. Therefore, in the same way as for the other models, the values of $\mathrm{Re}_{\mathrm{QU}}$ and γ_c^* can be calculated. Since D, ρ and μ_∞ are constant, the different Re values essentially correspond to different inlet flow rates, the mean value of which is U_∞.

The boundary conditions are constant velocity profile and pressure at the inlet and no-slip condition at the walls. At the outlet boundary the pressure and velocity are derived by extrapolation from the inner nodes. The velocity profile at the inlet is regarded to be that of the fully developed flow in a straight tube and can be derived analytically for Newtonian and Power-Law models. Due to the complex kind of the equations for the Quemada and Casson models, the fully developed flow used as inlet condition for each of these cases is calculated numerically similarly as in [12].

3 NUMERICAL METHOD

The code used for the calculations incorporates the finite volume method with collocated arrangement of variables on curvilinear grids and has been used in the past for 2D simulations [7, 12]. For coupling the momentum and continuity equations the pressure-correction method in conjunction with the SIMPLE scheme is applied. The newest feature is the incorporation of the QUICK differencing scheme for the approximation of the convection terms in order to avoid the diffusive effects of the low order schemes. Furthermore, the code enables also multi-block computations, which are useful in order to cope with the two-block grid structure of the current computational domain (Fig. 2).

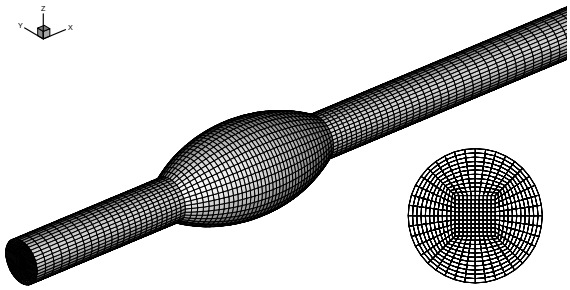

Fig. 2: 3D grid with cross-section.

The grid used in the computations consists of hexahedral elements and is based on multiblock structure with an inner block of rectangular cross section encircled by the outer block. Furthermore, the grid is locally refined near at the dilated segment so that the flow disturbances caused by the bulge are captured in more detail. A gird refinement study is also contacted

and three grid resolutions were tested namely grid *i* with 39345 control volumes (CVs), grid *ii* with 77108 CVs and grid *iii* with 104160 CVs. The results for grids *ii* and *iii* were very close and therefore grid *ii* is used for all further computations of this study.

4 RESULTS AND DISCUSION

Computations are contacted for three different Re numbers and three different aneurysm-shapes i.e. values of a in (8) so that the effects of the three blood models on important flow aspects such as the flow field and WSS distribution are determined. The effect of different Re numbers was studied for a=0.55 whereas the effect of the model shape was studied for Re=300. From a value of Re the velocity U_∞ is calculated from Re_{CA} and then used to calculate the rest of the parameters in (2), (3) and (4). Therefore the intercomparison between the models for a specific value of Re implies intercomparison for the same inlet flow rate.

4.1 Effects of Re number

The flows for all models corresponding to Re=300, 900 and 1500 are simulated assuming a=0.55 width of aneurysm. This range of Re numbers covers realistic flow conditions in the abdominal aorta [3, 13]. No indication of asymmetry of flow exists as regards to the axis of the tube so the results are presented corresponding to a random plane containing the axis.

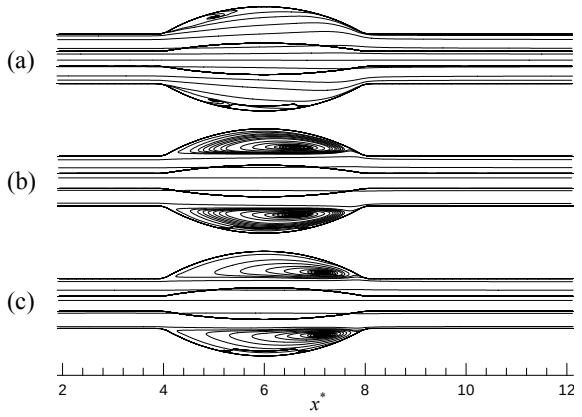

Fig. 3: Streamlines for Casson-based flow for (a) Re=300; (b) Re=900; (c) Re=1500 and width of aneurysm a=2.1.

The streamline patterns for the Casson model are shown in Figure 3 where the flow is regarded from left to right. The flow for Re=300 is almost fully attached and the recirculation zone is barely formed. For Re=900 the recirculation zone is covering the dilated segment whereas the core flow does not expand within the bulge as for Re=300. As Re increases further (Re=1500) the area of the recirculation zone remains unaltered whereas the vortex center moves downstream towards the exit from the aneurysm.

From the pressure-difference (ΔP) between inlet and outlet (Table 1) one can see that all non-Newtonian models cause higher pressure-difference than the Newtonian case and that implies that a specific pressure difference would induce lower flow rates for the non-Newtonian models. In particular the highest ΔP is induced by the Power-Law model followed by the Casson and then the Quemada models. The change from Re=300 to Re=900 seems to induce approximately the same rise to ΔP as the change from Re=900 to Re=1500 for all models. Furthermore, the difference between ΔP values for every model at a specific Re seems to be the same for all three Re values.

The distribution of the WSS is one of the most important flow aspects due to its direct relevance to atherosclerosis formation [1]. The maximum (τ_W^{max}) and minimum (τ_W^{min}) values of the distribution are shown in Table 2 for all models. For Re=300 the values of τ_W^{min} are very close for all models and similar to the Newtonian case whereas the values of τ_W^{max} are highest for the Power-Law followed gradually by the Casson and the Quemada models. All aforementioned values of τ_W^{max} are substantially higher than for the Newtonian case. As far as τ_W^{min} is concerned the same yields for higher values of Re whereas the increase of Re induces lower values of τ_W^{min} for the Newtonian case compared to the other models for which the values of τ_W^{min} are very close.

4.2 Effects of aneurysm growth

The flows for all models corresponding to Re=300 and aneurysm width equal to a=0.25, a=0.40 and a=0.55 are simulated. The streamlines for the Casson model in Figure 4 show the effects that the degree of aneurysm-width has on the flow field.

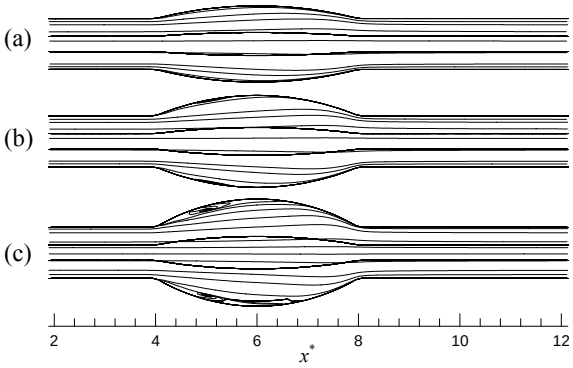

Fig. 4: Streamlines for Casson-based flow for different aneurysm widths (a) a=0.25; (b) a=0.40; (c) a=0.55 and Re=300.

It can be seen that for a=0.25 the flow is fully attached and the recirculation zone forms progressively for a>0.4. As shown in Table 1 the severity of the bulge shows no effect on the pressure drop (ΔP) for any of the models. ΔP remains highest for the Power-Law model followed gradually by the Casson, Quemada and Newtonian models but the increase of dilation leaves ΔP for every model virtually unaffected. Taking into account that the pressure difference is directly related to the integral of the WSS on the entire area of the wall, one should not expect considerable effects of the bulge

increase on the WSS distribution. Indeed, as can also be seen in Table 2, τ_W^{max} remains highest for the Power-Law model followed gradually by the Casson, Quemada and Newtonian models but the increase of dilation leaves both τ_W^{max} and τ_W^{min} for every model barely affected.

		Newtonian	Casson	Power-Law	Quemada
a=0.55	Re=300	5.43	12.21	13.97	9.85
a=0.55	Re=900	16.96	27.83	34.10	24.33
a=0.55	Re=1500	29.70	43.52	51.52	38.91
a=0.40	Re=300	5.43	12.23	13.99	9.86
a=0.25	Re=300	5.43	12.27	14.05	9.89

Table 1: Pressure difference (in N/m^2) for the various cases.

		Newtonian		Casson		Power-Law		Quemada	
a	Re	τ_W^{min}	τ_W^{max}	τ_W^{min}	τ_W^{max}	τ_W^{min}	τ_W^{max}	τ_W^{min}	τ_W^{max}
0.55	300	-0.012	0.132	-5.32e-3	0.258	-0.012	0.297	-0.012	0.219
0.55	900	-0.126	0.418	-0.082	0.653	-0.093	0.774	-0.094	0.577
0.55	1500	-0.297	0.696	-0.274	0.983	-0.298	1.162	-0.290	0.886
0.40	300	-7.21e-3	0.122	6.08e-3	0.238	-5.28e-3	0.272	-5.61e-3	0.201
0.25	300	-4.30e-3	0.108	0.022	0.209	0.016	0.240	9.54e-3	0.176

Table 2: Minimum and maximum wall shear-stress (in N/m^2) for the various cases.

5 CONCLUSIONS

A study of the flow effects of three different blood rheological models namely the Casson, Power-Law and Quemada models in a three-dimensional model of an abdominal aortic aneurysm is presented. The flow field and wall shear-stress (WSS) distributions that each model induces for different Re number and degrees of aneurysm-growth is investigated and results show that there are marked differences between simulating the blood as Newtonian and as non-Newtonian fluid. Furthermore, the Power-Law model exhibits the highest values of maximum wall shear stress (τ_W^{max}) and pressure drop (ΔP) compared to the other models whereas the values of the minimum wall shear stress (τ_W^{min}) are very close for all models. In addition the increase of Re induces a more rapid increase of τ_W^{max} for the Power-Law model compared to the rest of the models whereas the increase in aneurysm bulging has virtually no effect on neither ΔP nor the WSS distribution on any of the models. Conclusively the Power-Law model exhibits the highest sensitivity to any parametric change followed gradually by the Casson and Quemada models.

ACKNOWLEDGEMENT

The financial support by the Greek General Secretariat for Research and Technology under the contract 01EP24 is gratefully acknowledged.

REFERENCES

[1] D.N. Ku. Blood flow in arteries. *Annual Review of Fluid Mechanics* **29**, 399-434, 1997.

[2] S.C.M. Yu., W.K. Chan, B.T.H. Ng, L.P. Chua. A numerical investigation of the steady and pulsatile flow characteristics in axi-symmetric abdominal aortic aneurysm models with some experimental evaluation. *Journal of Medical Engineering & Technology*, **23**, 228-239, 1999.

[3] S.C.M. Yu. Steady and pulsatile flow studies in abdominal aortic aneurysm models using particle image velocimetry. *Int. Journal of Heat and Fluid Flow*, **21**, 74-83, 2000.

[4] C.J. Egelhoff, R.S. Budwig, D.F Elger, T.A. Khraishi, K.H. Johansen. Model studies of the flow in abdominal aortic aneurysms during resting and exercise conditions. *J. Biomechanics*, **32**, 1319-1329, 1999.

[5] A.N Salsac, S.R. Sparks, J.C. Lasheras. Hemodynamic changes occurring during progressive enlargement of abdominal aortic aneurysms. *Annals Vasc .Surg.*, **18**, 14-21, 2004.

[6] N. Viswanath, C.M. Rodkiewicz, S. Sajac. On the abdominal aortic aneurysms: pulsatile state considerations. *Medical Engineering and Physics*, **19**, 343-351, 1997.

[7] P. Neofytou and D. Drikakis. Effects of blood models on flows through a stenosis. *Int. J. Num. Meth. Fluids*, **43**, 597-635, 2003.

[8] F. J. Walburn and D. J. Schneck. A constitutive equation for whole human blood. *Biorheology*, **13**, 201-210, 1976.

[9] D. Quemada. Rheology of Concentrated Disperse systems III. General features of the proposed non-newtonian model. Comparison with experimental data. *Rheologica Acta*, **17**, 643-653, 1978.

[10] T. C. Papanastasiou. Flow of materials with yield. *Journal of Rheology*, **31**, 385-404, 1987.

[11] S. E. Charm, W. McComis and G. Kurland. Rheology and structure of blood suspension. *J. Appl. Physiol*, **19**, 127-133, 1964.

[12] P. Neofytou and D. Drikakis. Non-Newtonian flow instability in a channel with a sudden expansion. *J. Non-Newt. Fluid Mech.*, **111**, 127-150, 2003.

[13] R. Budwig, D. Elger, H. Hooper, J. Slippy. Steady flow in abdominal aortic aneurysm models. *ASME J. Biomechanical Engng* **115**, 418-423, 1993.